https://doi.org/10.15255/KUI.2022.048
KUI-15/2023
Original scientific paper
Received August 10, 2022
Accepted December 7, 2022

Multicomponent Adsorption Capacity Forecasting Based on Support Vector Machine with Dragonfly Algorithm

R. Moumen,[a,b] *M. Laidi*,[b*] *S. Hanini*,[b] *M. Hentabli*,[b,c] and *A. Ibrir*[b]

[a] Djilali Bounaama University of Khemis Miliana, Algeria
[b] Laboratory of Biomaterials and Transfer Phenomena, University of Médéa, Algeria
[c] Quality Control Laboratory, SAIDAL Complex, Médéa Unit, Médéa, Algeria

Abstract

The predictability of the adsorption capacity of the multicomponent adsorption system was modelled using Support Vector Machine (SVM). Two SVM models were built and compared. In the first model, the SVM method was used with an already built-in optimisation algorithm. However, in the second model, the SVM method was used by means of a very recent and efficient optimisation algorithm: the Dragonfly Algorithm (DA).

The models' accuracy was evaluated by three well-established statistical metrics (root mean squared error RMSE, determination coefficient R^2, and correlation coefficient R). The used data were collected from previous experimental papers published in literature containing all kinds of pollutants, such as heavy metal ions, dyes, and organic compounds, and different natural/synthetic adsorbents. The dataset contained five important variables with 1023 points; the variables were divided into four inputs (molecular weight, equilibrium concentrations of adsorbate, specific area of adsorbent, and temperature), and one output (adsorption capacity at equilibrium). The data were divided using the holdout function into two subsets (80 % for training set, and 20 % for test set). The programming stage was carried out using MATLAB software.

The results showed that the optimised DA-SVM model with RBF-Gaussian kernel function had good ability for global search combined with high prediction accuracy, with $R^2 = 0.997$, $R = 0.998$, and RMSE = 2.539.

The obtained model can be used to predict the efficiency of the adsorption system, and provides a tool for process optimisation responding to changes in operating conditions. A new graphical user interface (GUI) was developed with MATLAB GUI to estimate accurately the desired responses by using the best DA-SVM model.

Keywords

Multicomponent adsorption, MATLAB GUI, pollutants, support vector regression, Dragonfly algorithm

1 Introduction

Several separation techniques have been used to study the removal of different pollutants from water , among these methods being multicomponent adsorption.[1] This latest technique has attracted the interest of many industrial sectors because of its simplicity, high efficiency, and cost-effectiveness.[2–6]

Multicomponent adsorption equilibrium is complex due to the nonlinear relationships between dependent variables and the nature of the interactions between the adsorbent and the adsorbate (synergism, antagonism or non-interaction).[7] The chemical species are adsorbed at the same time with a different degree of competition, depending on several thermo-physicochemical and morphological parameters[8] In this sense, different theoretical and empirical models (kinetics such as pseudo-first-order, pseudo-second-order, liquid film diffusion and isotherms such as competitive Langmuir, Freundlich, Temkin, Dubinin–Radushkevich and Elovich)[9] have been proposed in literature to model this phenomenon. However, the application of these models is limited because they are established based on some restrictive assumptions about the physicochemical nature that affects the adsorption system.[10] Due to this complexity, machine learning algorithms have emerged as a powerful tool, compared to other classical methods, to tackle the nonlinear relationships directly from samples with no previous knowledge of the chemical or physical nature that affects the system.[10–13]

Different machine learning algorithms were used in the literature as an advanced mathematical tool to model the adsorption capacity of single and multicomponent adsorption systems, such as: artificial neural network (ANN),[3,7,11–15] support vector machine (SVM).[12,15–17]

The SVM method can overcome some disadvantages of the ANN model, such as robustness, and avoid the result of falling into local optimum.[18] However, the SVM's parameters are tuned using a built-in optimisers, which are generally selected by trial and error method.[18] This method causes troublesome prediction and large error.[18] Therefore, many methods have been proposed for improving parameter optimisation. Published in literature is a new, simple, and effective optimisation method called dragonfly,[19] which combines the SVM's parameters as the solution position of DA, and keeps the computing performance of the algorithm as the current fitness value of DA, and then iterates through those parameters to obtain the optimal location of the dragonfly, *i.e.*, the best parameters of the SVM.[18]

* Corresponding author: Prof Maamar Laidi, PhD
Email: laidi.maamar@univ-medea.dz

To the best our knowledge, no research has been published on the development of only one model capable of predicting the adsorption capacity based on any set of pollutants (heavy metals, dyes, pharmaceuticals, hydrocarbons, organic, and inorganic matter).

Therefore, the aim of this study was to use a novel hybrid DA-SVM algorithm for hyperparameters optimisation, to obtain the best prediction model in terms of statistical metrics for modelling the multicomponent adsorption capacity at equilibrium; this model can predict the adsorption capacity of ternary adsorption systems of different types of pollutants.

2 Dataset selection

The experimental data of this study were collected from a large body scientific literature. Table 1 represents the affecting parameters.

Table 1 – Statistical description of the dataset

Variable category	Variables			Unit
inputs	molecular weight of each pollutant	M_w	M_{w1}	g mol^{-1}
			M_{w2}	
			M_{w3}	
	specific area of adsorbent	A_s		m^2 g^{-1}
	temperature	T		°C
	concentrations	c_e	c_{e1}	mg l^{-1}
			c_{e2}	
			c_{e3}	
outputs	equilibrium adsorption capacity of each adsorbent	q_e	$q_{e,1}$	mg g^{-1}
			$q_{e,2}$	
			$q_{e,3}$	

The literature and the number of data used for each system are given in Table 2. The dataset was collected from various published papers; each paper contained different ternary competitive adsorption systems on different adsorbents. The published papers reported single or competitive adsorption like in binary or ternary systems. In this work, we collected only the ternary competitive adsorption from graphs using digitiser software. The three metals or antibiotics shown in Table 2 represent the three pollutants to be removed from the aqueous solution.

3 SVM modelling approach

The SVM algorithm was first proposed by *Cortes and Vapnik* in 1995.[53] The SVM algorithm presents some advantages as follows:

- It can model complex nonlinear behaviours,
- Potential for implementation in regression,
- It can deal with missing data, *etc*.

The SVM algorithm uses the trial and error optimisation method to tune its parameters. Therefore, some disadvantages can be encountered, such as low efficiency, accuracy, and speed of calculation. To overcome these problems, recent optimisation methods have been used to tune the SVM parameters, namely, Genetic algorithm (GA), Particle swarm optimisation (PSO),[54] Cuckoo optimisation algorithm (COA), Artificial Bee Colony (ABC), Simulated annealing (SA),[55] Ant Colony Optimisation (ACO),[56] Grid search, Firefly algorithm (FFA), and Dragonfly algorithm (DA).[57] A detailed theory of SVM has been explained by numerous researchers.[58] The output expression of the SVM model can be written by Eq. (1):

$$f(x) = w^{T} \cdot \varnothing(x) + b \tag{1}$$

where w and b are the weight and bias vector, respectively, $\varnothing(x)$ represents the nonlinear mapping transfer function, which maps x into higher dimensional feature space.

To obtain w, it is compulsory to tune the following regularised function, which can be expressed as in expression (2), with the constraint of expressions (3)–(4) and Eq. (5):

$$\min\left(\frac{1}{2}w^2 + C\sum_{n=1}^{N}\left(\xi_i - \xi_i^*\right)\right) \tag{2}$$

$$f(x_i) - \left(w^{T} \cdot \varnothing(x_i) + b\right) \leq +\xi_i,\ i = 1, 2, 3, \ldots, N \tag{3}$$

$$\xi_i, \xi_i^* \geq 0,\ i = 1, 2, 3, \ldots, N \tag{4}$$

$$f(x) = \sum_{i=1}^{N}\left(\delta_i - \delta_i^*\right) \cdot K(x, x_i) + b \tag{5}$$

ψ is equivalent to the function approximation accuracy placed on the training data samples.[15] C is the capacity parameter, ξ_i and ξ_i^* represent the positive slack variables.[15] K is a kernel function defined by an inner product of the nonlinear transfer function; the most used kernel function is the Gaussian Radial Basis function (RBF), which is given by Eq. (6):

$$k(x_i.x_j) = \exp\left(-\frac{\left|x_i - x_j\right|^2}{2\sigma^2}\right),\ \sigma \in \mathbb{R} \tag{6}$$

where σ is the width of RBF function.

The dragonfly algorithm is a nature-inspired algorithm that can overcome all shortcomings presented by other optimisation algorithms in the light of high efficiency, rapid convergence, less computational complexity, and better capability of determining the global optima.

There is a connection between the accuracy of the SVM model and C, ε, and σ. The GWO has been employed in

Table 2 – Dataset of mixture adsorbate in aqueous solution adsorbed on different adsorbents

Ref.	Adsorbate	Adsorbent	Dataset size	Ref.	Adsorbate	Adsorbent	Data set size
20	$Cd^{2+}+Cu^{2+}+Pb^{2+}$	activated carbon	24	21	$Cd^{2+}+Cu^{2+}+Zn^{2+}$	biochar	15
		peanut shell					
		sawdust					
22	$Cd^{2+}+Ni^{2+}+Co^{2+}$	nanotubes	33	23	$Zn^{2+}+Cu^{2+}+Pb^{2+}$	biochar	18
24	$Cu^{+2}+Pb^{+2}+Hg^{+2}$	activated carbon	39			magnetic biochar	18
25	$Pb^{2+}+Cu^{2}+Zn^{2+}$	NaX zeolite	18	26	$Cd^{2+}+Cu^{2+}+Zn^{2+}$	natural sediment	45
	$Pb^{2+}+Cd^{2+}+Cu^{2+}$		18	27	$Cu^{2+}+Zn^{2+}+Hg^{2+}$	calcined magnetic biochar	12
	$Cd^{2+}+Cu^{2+}+Zn^{2+}$		18			calcined biochar	12
28	$Pb^{2+}+Hg^{2+}+Cr^{2+}$	activated sludge	51	29	$Cu^{2+}+Zn^{2+}+Cd^{2+}$	cabbage waste	11
					$Cu^{2+}+Zn^{2+}+Pb^{2+}$		19
					$Cu^{2+}+Pb^{2+}+Cd^{2+}$		22
30	$Cr^{3+}+Pb^{2+}+Cd^{2+}$	dead anaerobic biomass (DAB)	30	31	$Pb^{2+}+Cu^{2+}+Cd^{2+}$	locally porcelanite	39
32	$Ni^{2+}+Cu^{2+}+Pb^{2+}$	phosphoric acid activated carbon	18	33	$Ni^{2+}+Cu^{2+}+Cd^{2+}$	phosphate rocks (PR)	36
34	$Cu^{+2}+Zn^{+2}+Pb^{+2}$	polypropylene fibre	30	35	$Ni^{2+}+Cd^{2+}+Pb^{2+}$	mesoporous and nano-mesoporous silica (nano- MCM-41)	15
36	$Pb^{2+}+Zn^{2+}+Cd^{2+}$	Al-SM	27	37	$Pb^{2+}+Hg^{2+}+Cd^{2+}$	biosorption	6
	$Pb^{2+}+Zn^{2+}+Cd^{2+}$	ASM	27		$Pb^{2+}+As^{5+}+Hg^{2+}$		6
					$Pb^{2+}+As^{5+}+Cr^{3+}$		6
					$As^{5+}+Hg^{2+}+Cr^{3+}$		6
38	$Pb^{2+}+Zn^{2+}+Cd^{2+}$	peat	24	39	Remazol reactive yellow+ Remazol reactive black+ Remazol reactive red	activated carbon	15
40	Phenanthrene + Naphthalene + Naphthol	nanotube carbon	15	41	Methylene blue+ Malachite green+ Congo red	activated carbon	12
42	Congo red+ Crystal violet+ Brilliant green	alginic biopolymer composite	30	43	Safranine O+ Brilliant green+ Methylene blue	pine cone modified	45
44	Acetaminophen+ Diclofenac+ Tetracycline	argil	54	45	Methylene blue+ Crystal violet+ Congo red	argil	18
46	Tetracycline+ Amoxicillin+ Ciprofloxacin	pistachio shell powder	30	47	Congo red+ Brilliant green+ Methylene blue	alginic biopolymer composite	30
48	Carbamazepine+ Paroxetine+ Oxazepam	commercial activated carbon	18	49	Direct fast scarlet + Eosin Y+ Reactive violet K-3R	EPIDMA/bentonite	24
50	Ethanol+ Acetoin+ Acetic acid	resin	24	51	Trimellitic acid+ Hemimellitic acid+ Pyromellitic acid	cellulosic agricultural waste	15
52	Acetone+ Toluene + *n*-hexane	activated carbon	51				

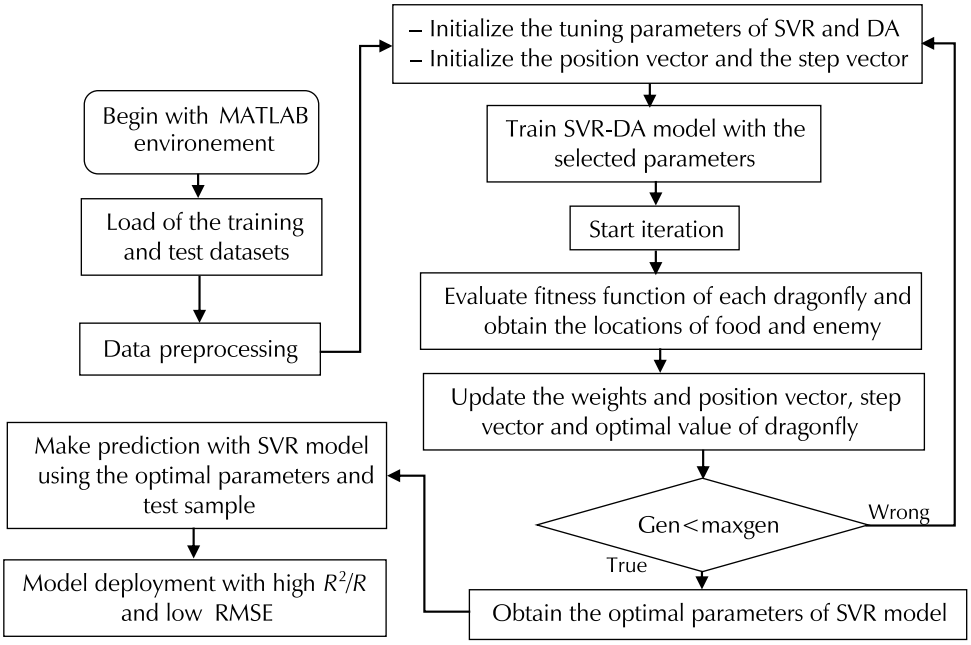

Fig. 1 – Schematic depiction of DA-SVM

this study to tune the aforementioned three SVM parameters. Fig. 1 illustrates the flowchart of the hybrid DA-SVM methodology model to be implemented in MATLAB software.

The DA algorithm was used to tune the SVM hyper-parameters (C, ε, σ) in the following search space, respectively ([10^{-3}−10^{3}], [10^{-3}−10^{3}], close to zero). The maximum iteration and search agents were fixed to 20 and 7, respectively, with RMSE as a fitness function. In this study, three kernel functions were tested ('Gaussian', 'linear', and 'polynomial').

4 Statistical evaluation and uncertainty in models

The performance of the best model was measured using three statistical metrics: R, R^2, and RMSE. These metrics can be expressed as follows:

$$\mathrm{RMSE} = \sqrt{\frac{1}{N}\sum_{i=1}^{n}\left(q_{e,i}^{\exp} - q_{e,i}^{\mathrm{cal}}\right)^2} \tag{7}$$

where $q_{e,i}^{\exp}$ and $q_{e,i}^{\mathrm{cal}}$ are the experimental and the calculated adsorption capacities. Coefficients R and R^2 are also employed to confirm the accuracy of the best developed models, the R^2 can be expressed by the following equation:[59–61]

$$R^2 = 1 - \frac{\sum_{i=1}^{n}\left(q_{e,i}^{\exp} - q_{e,i}^{\mathrm{cal}}\right)^2}{\sum_{i=1}^{n}\left(q_{e,i}^{\exp} - \overline{q_e^{\exp}}\right)^2} \tag{8}$$

where $\overline{q_e^{\exp}}$ is the mean of the experimental values and n is number of data sample.

Table 3 represents the performances of each model when modelling the adsorption phenomena in terms of RMSE, R, and R^2. Table 3 presents the values of the DA-SVM model performance, the correlation coefficient, and the root mean square error.

Table 3 – Statistical parameters of the DA-SVM model for the global stage

Method	Kernel Function	R	R^2	RMSE / mg g^{-1}
DA-SVM	linear	0.405	0.164	42.550
	polynomial	0.564	0.318	39.000
	RBF-Gaussian	**0.998**	**0.997**	**2.540**
SVM	RBF-Gaussian	0.985	0.9693	7.525

In this study, the dataset was divided into two subsets, using 80 % for training set, and 20 % for the test set. Diverse kernel functions have been tested: linear, polynomial, RBF, and Gaussian. The results of the optimised hyper-parameters of the SVM model are summarized in Table 4. The RBF-Gaussian kernel function gave the best results, yielding the lowest error and highest correlation coefficient among all kernel functions.

Scatter plots show the comparison between measured and predicted adsorption capacity values obtained using the best model for the training, whereas testing dataset is

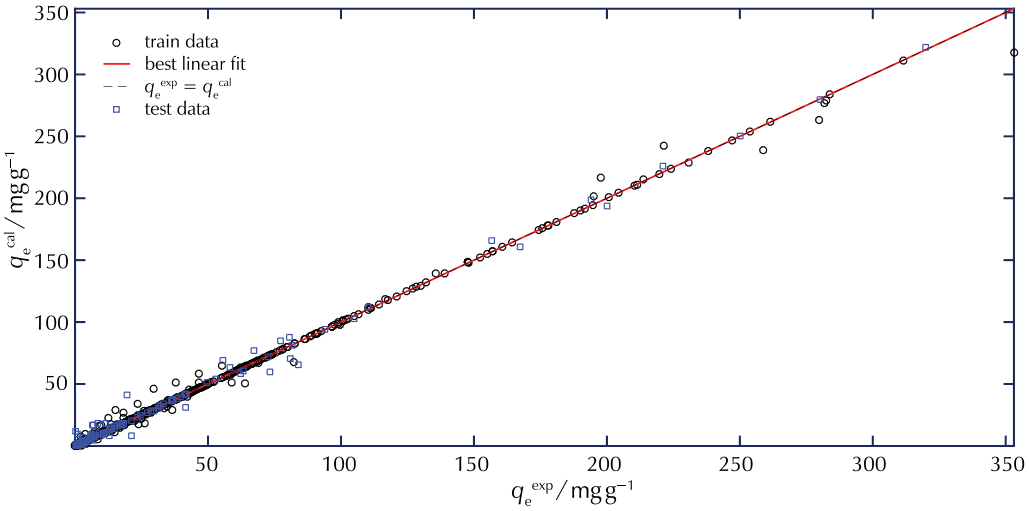

Fig. 2 – Observed *vs* predicted adsorption capacity values for the global stage

Table 4 – Details of the optimised hyper parameters for the SVM model

Method	Kernel function	*C*	Kernel scale sigma (σ)	Epsilon (ε)	Quantity of support vectors
DA-SVM	linear	640	–	1950	921
	polynomial	327.100	–	1050	921
	RBF-Gaussian	**500**	**0.0182**	**22.500**	**921**
SVM	RBF-Gaussian	640	0.100	518.700	921

shown in Fig. 2. The correlation and the determination coefficient were found to be, respectively, 0.998 and 0.997 for the DA-SVR model using RBF-Gaussian as the kernel function. Hence, the obtained DA-SVM with RBF-Gaussian kernel function is statistically significant. The MSE was used as a fitness function to evaluate how close the solution was to the optimal solution.

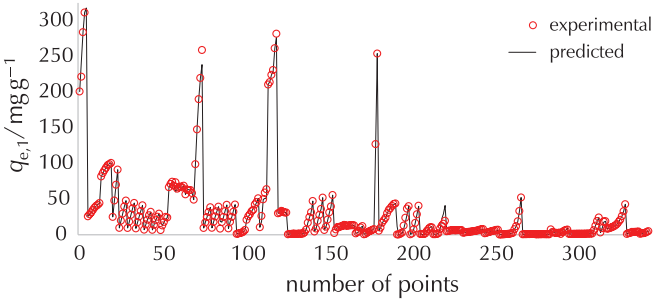

Fig. 3 – Predicted *vs* experimental adsorption capacity for $q_{e,1}$ (mg g^{-1})

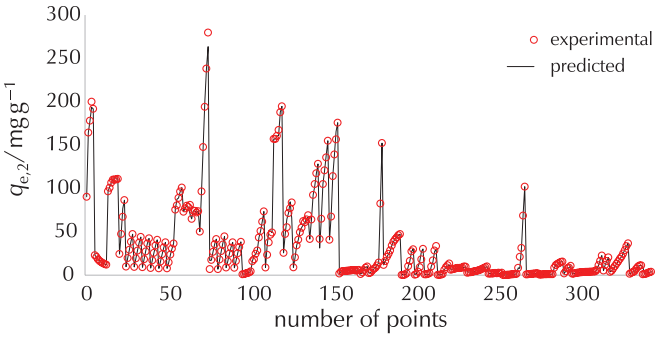

Fig. 4 – Predicted *vs* experimental adsorption capacity for $q_{e,2}$ (mg g^{-1})

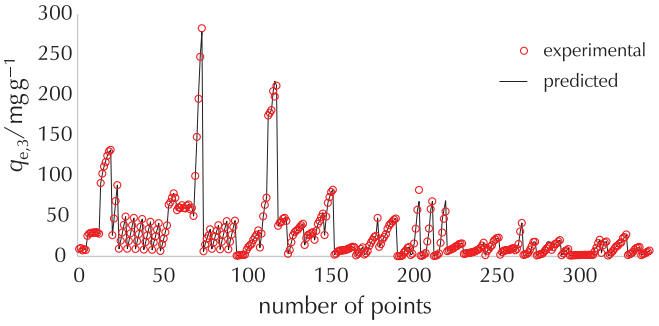

Fig. 5 – Predicted *vs* experimental adsorption capacity for $q_{e,3}$ (mg g^{-1})

Figs. 3 to 5 again confirmed the accuracy of the DA-SVM model between experimental and predicted ternary adsorption capacity ($q_{e,i}$, i = 1, 2, 3). These figures showed that the predicted values followed the trend of the nonlinear experimental values. The developed model presented very low values of RMSE (2.540) for the global stage, and

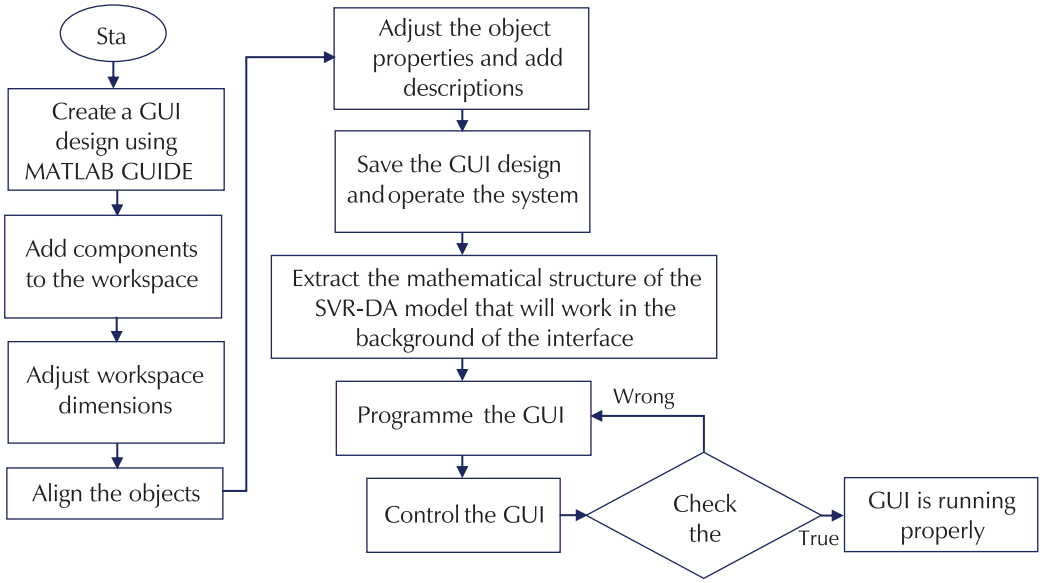

Fig. 6 – Constructing procedure for the GUI

high R^2 values of 0.997 for the three outputs. The results confirmed the high prediction ability of the developed model, and the possibility of being integrated in water treatment and purification unit.

5 MATLAB-based GUI

To provide a simple and convivial use of the optimal DA-SVR model in estimating the target values and avoiding dealing with the complex architecture of the model with many weights and biases, a practical GUI was designed with MATLAB R2018a GUI Toolbox. The constructing procedure of the GUI is presented in Fig. 6.

The GUI presented in Fig. 7 was built using the optimised model with high accuracy; the input parameters are written directly in the related textboxes whose descriptions are stated above the boxes. The inputs are then used with weights and biases of the optimised model to estimate the adsorption capacity of ternary systems as outputs in the range of the used inputs.

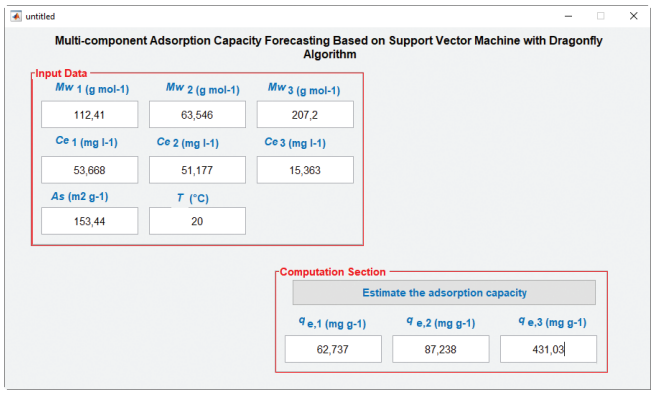

Fig. 7 – Implementation of the best model in GUI to estimate the target values

6 Conclusions

The efficiency of SVM and DA-SVM in the prediction of the adsorption capacity was evaluated in this work. Based on the statistical metrics evaluated, the accuracy of the models in terms of accuracy and precision was in this order: DA-SVM with RBF-Gaussian kernel function (model 1), SVM with RBF-Gaussian kernel function (model 2), DA-SVM with polynomial kernel function (model 3), and DA-SVM with linear kernel function (model 4). Model 4 had significantly high *RMSE* (42.550 mg $^{g-1}$) compared to model 3 (39 mg $^{g-1}$), model 2 (7.525 mg $^{g-1}$), and model 1 (2.540 mg $^{g-1}$).

The developed DA-SVM model can be used to predict the adsorption capacity of any ternary pollutant system (heavy metals, dyes, pharmaceuticals, hydrocarbons, organic, and inorganic matter) involved in water treatment and purification. In order to simplify the use of the obtained model, a single MATLAB-based GUI was developed based on best model's parameters that could be used for response prediction with high accuracy.

List of abbreviations

RMSE – root mean squared error
MSE – mean squared error
R^2 – determination coefficient
R – correlation coefficient
$q_{e,i}$ – capacity of adsorption of the component *i*

$q_{e,i}^{exp}$ – experimental value of the capacity of adsorption

$q_{e,i}^{cal}$ – predicted value of the capacity of adsorption

$\overline{q_e^{exp}}$ – mean of the experimental values

N – number of data set

M_{wi} – molecular weight of the component i

c_{ei} – concentration of the component i

A_s – specific area of the adsorbent

T – temperature

w – weight matrix and w^T is its transpose

b – bias vector

$\varnothing(x)$ – nonlinear mapping transfer function, which maps x into higher dimensional feature space

C – capacity parameter

σ – width of RBF function

ε – insensitive loss function

ξ_i and ξ_i^* – positive slack variables

δ_i and δ_i^* – Lagrange multipliers

ψ – equivalent to the function approximation accuracy placed on the training data samples

K – kernel function

References
Literatura

1. *V. C. Srivastava, I. D. Mall, I. M. Mishra*, Modelling individual and competitive adsorption of cadmium(II) and zinc(II) metal ions from aqueous solution onto bagasse fly ash, Sep. Sci. Technol. **41** (2006) 2685–2710, doi: https://doi.org/10.1080/01496390600725687.
2. *M. Gutierrez, H. R. Fuentes*, Modeling adsorption in multicomponent systems using a Freundlich-type isotherm, J. Contam. Hydrol. **14** (1993) 247–260, doi: https://doi.org/10.1016/0169-7722(93)90027-P.
3. *P. S. Pauletto, S. F. Lütke, G. L. Dotto, N. P. G. Salau*, Forecasting the multicomponent adsorption of nimesulide and paracetamol through artificial neural network, Chem. Eng. J. **412** (2021) 127527, doi: https://doi.org/10.1016/j.cej.2020.127527.
4. *Z.-R. Liu, S.-Q. Zhou*, Adsorption of copper and nickel on Na-bentonite, Process Saf. Environ. Prot. **88** (2010) 62–66, doi: https://doi.org/10.1016/j.psep.2009.09.001.
5. *L. Vrsalović, S. Gudić, L. Terzić, I. Ivanić, S. Kožuh, M. Gojić, E. E. Oguzie*, Intergranular Corrosion of Cu-Al-Ni Alloy in 0.5 mol dm^{-3} H_2SO_4 Solution, J. Chem. Chem. Eng. **69** (2020) 457–464, doi: https://doi.org/https://doi.org/10.15255/KUI.2020.022.
6. *M. Ostojčić, S. Brkić, M. Tišma, B. Zelić, S. Budžaki*, Membrane filtration as an environmentally friendly method for crude biodiesel purification, J. Chem. Chem. Eng. **69** (2020) 175–181, doi: https://doi.org/https://doi.org/10.15255/KUI.2019.049.
7. *P. S. Pauletto, J. O. Gonçalves, L. A. A. Pinto, G. L. Dotto, N. P. G. Salau*, Single and competitive dye adsorption onto chitosan–based hybrid hydrogels using artificial neural network modeling, J. Colloid Interface Sci. **560** (2020) 722–729, doi: https://doi.org/10.1016/j.jcis.2019.10.106.
8. *A. Maleki, B. Hayati, F. Najafi, F. Gharibi, S. W. Joo*, Heavy metal adsorption from industrial wastewater by PAMAM/TiO_2 nanohybrid: Preparation, characterization and adsorption studies, J. Mol. Liq. **224** (2016) 95–104, doi: https://doi.org/10.1016/j.molliq.2016.09.060.
9. *S. V. Manjunath, R. Singh Baghel, M. Kumar*, Antagonistic and synergistic analysis of antibiotic adsorption on Prosopis juliflora activated carbon in multicomponent systems, Chem. Eng. J. **381** (2020), doi: https://doi.org/10.1016/j.cej.2019.122713.
10. *W. Zhang, W. Huang, J. Tan, D. Huang, J. Ma, B. Wu*, Modeling, optimization and understanding of adsorption process for pollutant removal via machine learning: Recent progress and future perspectives, Chemosphere **311** (2023), doi: https://doi.org/10.1016/j.chemosphere.2022.137044.
11. *M. R. Gadekar, M. M. Ahammed*, Modelling dye removal by adsorption onto water treatment residuals using combined response surface methodology-artificial neural network approach, J. Environ. Manage. **231** (2019) 241–248, doi: https://doi.org/10.1016/j.jenvman.2018.10.017.
12. *A. Yettou, M. El Bey, M. Laidi, S. Hanini, M. Hentabli, O. Khaldi, A. Mihoub*, Multicomponent adsorption modelling using ANN, LS-SVR, and SVR approach, J. Chem. Chem. Eng. **70** (2021) 509–518, doi: https://doi.org/https://doi.org/10.15255/KUI.2020.071.
13. *M. El bey, M. Laidi, A. Yettou, S. Hanini, A. Ibrir, M. Hentabli, H. Ouldkhaouaa*, Practical artificial neural network tool for predicting the competitive adsorption of dyes on Gemini Polymeric Nanoarchitecture, J. Chem. Chem. Eng. **70** (2021) 481−488, doi: https://doi.org/https://doi.org/10.15255/KUI.2020.069.
14. *Y. Mesellem, A. Abdallah el Hadj, M. Laidi, S. Hanini, M. Hentabli*, Artificial neural network modelling of multi-system dynamic adsorption of organic pollutants on activated carbon, J. Chem. Chem. Eng. **70** (2021) 1–12, doi: https://doi.org/https://doi.org/10.15255/KUI.2020.011.
15. *Y. Mesellem, A. A. El Hadj, M. Laidi, S. Hanini, M. Hentabli*, Computational intelligence techniques for modeling of dynamic adsorption of organic pollutants on activated carbon, Neural Comput. Appl. **2** (2021), doi: https://doi.org/10.1007/s00521-021-05890-2.
16. *M. Ghaedi, A. M. Ghaedi, M. Hossainpour, A. Ansari, M. H. Habibi, A. R. Asghari*, Least square-support vector (LS-SVM) method for modeling of methylene blue dye adsorption using copper oxide loaded on activated carbon: Kinetic and isotherm study, J. Ind. Eng. Chem. **20** (2014) 1641–1649, doi: https://doi.org/10.1016/j.jiec.2013.08.011.
17. *R. Syah, M. H. Towfighi Naeem, R. Daneshfar, H. Dehdar, B. S. Soulgani*, On the prediction of methane adsorption in shale using grey wolf optimizer support vector machine approach, Petroleum **8** (2022) 264–269, doi: https://doi.org/10.1016/j.petlm.2021.12.002.
18. *Y. Feng, P. Zhang, M. Yang, Q. Li, A. Zhang*, Short term load forecasting of offshore oil field microgrids based on DA-SVM, Energy Procedia **158** (2019) 2448–2455, doi: https://doi.org/10.1016/j.egypro.2019.01.318.
19. *F. Meng, Q. Zou, Z. Zhang, B. Wang, H. Ma, H. M. Abdullah, A. Almalaq, M. A. Mohamed*, An intelligent hybrid wavelet-adversarial deep model for accurate prediction of solar power generation, Energy Reports **7** (2021) 2155–2164, doi: https://doi.org/10.1016/j.egyr.2021.04.019.
20. *X. Liu, X. Xu, X. Dong, J. Park*, Competitive adsorption of

heavy metal ions from aqueous solutions onto activated carbon and agricultural waste materials, Polish J. Environ. Stud. **29** (2020) 749–761, doi: https://doi.org/10.15244/pjoes/104455.

21. *J. H. Park, J. S. Cho, Y. S. Ok, S. H. Kim, S. W. Kang, I. W. Choi, J. S. Heo, R. D. Delaune, D. C. Seo*, Competitive adsorption and selectivity sequence of heavy metals by chicken bone-derived biochar: Batch and column experiment, J. Environ. Sci. Heal. – Part A **50** (2015) 1194–1204, doi: https://doi.org/10.1080/10934529.2015.1047680.
22. *A. Roy, J. Bhattacharya*, A binary and ternary adsorption study of wastewater Cd(II), Ni(II) and Co(II) by γ-Fe_2O_3 nanotubes, Sep. Purif. Technol. **115** (2013) 172–179, doi: https://doi.org/10.1016/j.seppur.2013.05.010.
23. *Q. Wu, S. Dong, L. Wang, X. Li*, Single and competitive adsorption behaviors of Cu^{2+}, Pb^{2+} and Zn^{2+} on the biochar and magnetic biochar of pomelo peel in aqueous solution, Water **13** (2021) 868, doi: https://doi.org/https://doi.org/10.3390/w13060868.
24. *J. Goel, K. Kadirvelu, C. Rajagopal*, Competitive sorption of Cu(II), Pb(II) and Hg(II) ions from aqueous solution using coconut shell-based activated carbon, Adsorpt. Sci. Technol. **22** (2004) 257–273, doi: https://doi.org/10.1260/0263617041503453.
25. *X. Fan, H. Liu, E. Anang, D. Ren*, Effects of electronegativity and hydration energy on the selective adsorption of heavy metal ions by synthetic nax zeolite, Materials **14** (2021), doi: https://doi.org/10.3390/ma14154066.
26. *L. Huang, Q. Jin, P. Tandon, A. Li, A. Shan, J. Du*, High-resolution insight into the competitive adsorption of heavy metals on natural sediment by site energy distribution, Chemosphere **197** (2018) 411–419, doi: https://doi.org/10.1016/j.chemosphere.2018.01.056.
27. *A. A. Oladipo, E. O. Ahaka, M. Gazi*, High adsorptive potential of calcined magnetic biochar derived from banana peels for Cu^{2+}, Hg^{2+}, and Zn^{2+} ions removal in single and ternary systems, Environ. Sci. Pollut. Res. **26** (2019) 31887–31899, doi: https://doi.org/10.1007/s11356-019-06321-5.
28. *A. H. Sulaymon, S. A. Yousif, M. M. Al-Faize*, Single-multicomponent biosorption of lead mercury chromium and arsenic onto activated sludge in batch and fixed-bed adsorber, Desalin. Water Treat. **53** (2015) 3499–3512, doi: https://doi.org/10.1080/19443994.2013.872054.
29. *M. A. Hossain, H. H. Ngo, W. S. Guo, L. D. Nghiem, F. I. Hai, S. Vigneswaran, T. V. Nguyen*, Competitive adsorption of metals on cabbage waste from multi-metal solutions, Bioresour. Technol. **160** (2014) 79–88, doi: https://doi.org/10.1016/j.biortech.2013.12.107.
30. *A. H. Sulaymon, S. E. Ebrahim, M. J. M-Ridha*, Competitive biosorption of Pb(II), Cr(III), and Cd (II) from synthetic wastewater onto heterogeneous anaerobic biomass in single, binary, and ternary batch systems, Desalin. Water Treat. **52** (2014) 5629–5638, doi: https://doi.org/10.1080/19443994.2013.813008.
31. *N. J. Hamadi, A. A. Mohammed, A. H. Ali*, Removal of Pb^{2+}, Cu^{2+} and Cd^{2+} metals from simulated wastewater in single and competitive system using locally porcelanite, Int. J. Eng. Sci. Res. Technol. **3** (2014) 245–257, doi: https://doi.org/10.1080/00986445.2013.823542
32. *M. M. Rahman, S. H. Samsuddin, M. F. Miskon, K. Yunus, A. M. Yusof*, Phosphoric acid activated carbon as borderline and soft metal ions scavenger, Green Chem. Lett. Rev. **8** (2015) 9–20, doi: https://doi.org/10.1080/17518253.2015.1058974.
33. *A. H. Ali*, Treatment of wastewater contaminated with dyes using modified low-cost adsorbents, Desalin. Water Treat. **140** (2019) 326–336, doi: https://doi.org/10.5004/dwt.2019.23513.
34. *D. Zhao, Z. Wang, S. Lu, X. Shi*, An amidoxime-functionalized polypropylene fiber: Competitive removal of Cu(II), Pb(II) and Zn(II) from wastewater and subsequent sequestration in cement mortar, J. Clean. Prod. **274** (2020) 123049, doi: https://doi.org/10.1016/j.jclepro.2020.123049.
35. *A. Heidari, H. Younesi, Z. Mehraban*, Removal of Ni(II), Cd(II), and Pb(II) from a ternary aqueous solution by amino functionalized mesoporous and nano mesoporous silica, Chem. Eng. J. **153** (2009) 70–79, doi: https://doi.org/10.1016/j.cej.2009.06.016.
36. *P. Parthasarathy, S. K. Narayanan*, Effect of hydrothermal carbonization reaction parameters on, Environ. Prog. Sustain. Energy **33** (2014) 676–680, doi: https://doi.org/10.1002/ep.
37. *A. H. Sulaymon, S. E. Ebrahim, S. M. Abdullah, T. J. Al-Musawi*, Removal of lead, cadmium, and mercury ions using biosorption, Desalin. Water Treat. **24** (2010) 344–352, doi: https://doi.org/10.5004/dwt.2010.1963.
38. *R. Balasubramanian, S. V. Perumal, K. Vijayaraghavan*, Equilibrium isotherm studies for the multicomponent adsorption of lead, zinc and cadmium onto Indonesian peat, Ind. Eng. Chem. Res. **48** (2009) 2093–2099, doi: https://doi.org/10.1021/ie801022p.
39. *Y. Al-Degs, M. A. M. Khraisheh, S. J. Allen, M. N. Ahmad, G. M. Walker*, Competitive adsorption of reactive dyes from solution: Equilibrium isotherm studies in single and multisolute systems, Chem. Eng. J. **128** (2007) 163–167, doi: https://doi.org/10.1016/j.cej.2006.10.009.
40. *X. Wang, S. Tao, B. Xing*, sorption and competition of aromatic compounds and humic acid on multiwalled carbon nanotubes, Environ. Sci. Technol. **43** (2009) 6214–6219, doi: https://doi.org/https://doi.org/10.1021/es901062t.
41. *Z. N. Garba, Z. U. Zango, A. A. Babando, A. Galadima*, Competitive adsorption of dyes onto granular activated carbon, J. Chem. Pharm. Res. **7** (2015) 710–717.
42. *M. Kumar, H. S. Dosanjh, H. Singh*, Magnetic zinc ferrite–alginic biopolymer composite: as an alternative adsorbent for the removal of dyes in single and ternary dye system, J. Inorg. Organomet. Polym. Mater. **28** (2018) 1688–1705, doi: https://doi.org/10.1007/s10904-018-0839-2.
43. *S. Debnath, N. Ballav, A. Maity, K. Pillay*, Competitive adsorption of ternary dye mixture using pine cone powder modified with β-cyclodextrin, J. Mol. Liq. **225** (2017) 679–688, doi: https://doi.org/10.1016/j.molliq.2016.10.109.
44. *A. Gómez-Avilés, L. Sellaoui, M. Badawi, A. Bonilla-Petriciolet, J. Bedia, C. Belver*, Simultaneous adsorption of acetaminophen, diclofenac and tetracycline by organo-sepiolite: Experiments and statistical physics modelling, Chem. Eng. J. **404** (2021), doi: https://doi.org/10.1016/j.cej.2020.126601.
45. *S. Bentahar, A. Dbik, M. El Khomri, N. El Messaoudi, A. Lacherai*, Adsorption of methylene blue, crystal violet and congo red from binary and ternary systems with natural clay: Kinetic, isotherm, and thermodynamic, J. Environ. Chem. Eng. **5** (2017) 5921–5932, doi: https://doi.org/10.1016/j.jece.2017.11.003.
46. *A. A. Mohammed, T. J. Al-Musawi, S. L. Kareem, M. Zarrabi, A. M. Al-Ma'abreh*, Simultaneous adsorption of tetracycline, amoxicillin, and ciprofloxacin by pistachio shell powder coated with zinc oxide nanoparticles, Arab. J. Chem. **13** (2019) 4629–4643, doi: https://doi.org/10.1016/j.arabjc.2019.10.010.
47. *M. Kumar, H. S. Dosanjh, H. Singh*, Surface modification of spinel ferrite with biopolymer for adsorption of cationic and anionic dyes in single and ternary dye system, Fibers Polym. **20** (2019) 739–751, doi: https://doi.org/10.1007/s12221-

019-8462-6.

48. *V. Calisto, G. Jaria, C. P. Silva, C. I. A. Ferreira, M. Otero, V. I. Esteves*, Single and multicomponent adsorption of psychiatric pharmaceuticals onto alternative and commercial carbons, J. Environ. Manage. **192** (2017) 15–24, doi: https://doi.org/10.1016/j.jenvman.2017.01.029.
49. *Q. Kang, W. Zhou, Q. Li, B. Gao, J. Fan, D. Shen*, Adsorption of anionic dyes on poly(epicholorohydrin dimethylamine) modified bentonite in single and mixed dye solutions, Appl. Clay Sci. **45** (2009) 280–287, doi: https://doi.org/10.1016/j.clay.2009.06.010.
50. *J. Wu, X. Ke, L. Wang, R. Li, X. Zhang, P. Jiao, W. Zhuang, Y. Chen, H. Ying*, Recovery of acetoin from the ethanol-acetoin-acetic acid ternary mixture based on adsorption methodology using a hyper-cross-linked resin, Ind. Eng. Chem. Res. **53** (2014) 12411–12419, doi: https://doi.org/10.1021/ie502105q.
51. *M. Laabd, A. El Jaouhari, M. Ait Haki, H. Eljazouli, M. Bazzaoui, H. Kabli, A. Albourine*, Simultaneous removal of benzene polycarboxylic acids from water by polypyrrole composite filled with a cellulosic agricultural waste, J. Environ. Chem. Eng. **4** (2016) 1869–1879, doi: https://doi.org/10.1016/j.jece.2016.03.015.
52. *I. Ushiki, Y. Sato, M. Ota, H. Inomata*, Multicomponent (binary and ternary) adsorption equilibria of volatile organic compounds (acetone, toluene, and n-hexane) on activated carbon in supercritical carbon dioxide, Ind. Eng. Chem. Res. **55** (2016) 2163–2173, doi: https://doi.org/10.1021/acs.iecr.5b04383.
53. *C. Cortes, V. Vapnik*, Support-vector networks, Mach. Learn. **20** (1995) 273–297, doi: https://doi.org/10.1007/BF00994018.
54. *R. Teimouri*, Optimization of residual stress field in ultrasonic assisted burnishing process, Int. J. Light. Mater. Manuf. **2** (2019) 346–354, doi: https://doi.org/https://doi.org/10.1016/j.ijlmm.2019.04.009.
55. *S. P. Khanghah, M. Boozarpoor, M. Lotfi, R. Teimouri*, Optimization of micro-milling parameters regarding burr size minimization via RSM and simulated annealing algorithm, Trans. Indian Inst. Met. **68** (2015) 897–910, doi: https://doi.org/https://doi.org/10.1007/s12666-015-0525-9.
56. *R. Teimouri, H. Baseri*, Optimization of magnetic field assisted EDM using the continuous ACO algorithm, Appl. Soft Comput. **14** (2014) 381–389.
57. *A. Zendehboudi, M. A. Baseer, R. Saidur*, Application of support vector machine models for forecasting solar and wind energy resources: A review, J. Clean. Prod. **199** (2018) 272–285, doi: https://doi.org/10.1016/j.jclepro.2018.07.164.
58. *I. O. Alade, M. A. Abd Rahman, Z. Abbas, Y. Yaakob, T. A. Saleh*, Application of support vector regression and artificial neural network for prediction of specific heat capacity of aqueous nanofluids of copper oxide, Sol. Energy **197** (2020) 485–490, doi: https://doi.org/https://doi.org/10.1016/j.solener.2019.12.067.
59. *M. Wei, X. Yang, P. Watson, F. Yang, H. Liu*, Development of QSAR model for predicting the inclusion constants of organic chemicals with α-cyclodextrin, Environ. Sci. Pollut. Res. **25** (2018) 17565–17574, doi: https://doi.org/10.1007/s11356-018-1917-2.
60. *M. Laidi, S. Hanini, A. El, H. Abdallah*, Novel approach for estimating monthly sunshine duration using artificial neural networks: a sase study, J. Sustain. Dev. Energy, Water Environ. Syst. **6** (2018) 405–414, doi: https://doi.org/https://doi.org/10.13044/j.sdewes.d6.0226.
61. *M. Iqbal, U. Ali, A. Ahmad, H.- Rehman, U. Ghani, T. Farid*, Relating groundwater levels with meteorological parameters using ANN technique, Measurement **166** (2020) 108163, doi: https://doi.org/10.1016/j.measurement.2020.108163.

SAŽETAK

Predviđanje kapaciteta višekomponentne adsorpcije metodom potpornih vektora uz algoritam Dragonfly

Riadh Moumen,[a,b] *Maamar Laidi*,[b*] *Salah Hanini*,[b] *Mohamed Hentabli* [b,c] i *Abdellah Ibrir*[b]

Višekomponentni adsorpcijski kapacitet modelirana je metodom potpornih vektora (SVM). Razvijena su i uspoređena dva SVM modela. U prvom modelu primijenjena je metoda SVM s već ugrađenim optimizacijskim algoritmom. U drugom modelu primijenjena je SVM metoda s Dragonfly algoritmom (DA) optimizacije. Točnost modela procijenjena je pomoću tri uvriježene statističke mjere: korijena srednje kvadratne pogreške RMSE, koeficijenta determinacije R^2 i koeficijenta korelacije R. Korišteni podatci o raznim onečišćivalima, poput iona teških metala, boja i organskih spojeva te različitim prirodnim/sintetskim adsorbensima prikupljeni su iz literaturno dostupnih znanstvenih radova. Skup podataka sadržavao je pet važnih varijabli s 1023 točke; 4 varijable bile su ulazne varijable (molekulska masa, ravnotežne koncentracije adsorbata, specifično područje adsorbensa i temperatura), a jedna izlazna (ravnotežni adsorpcijski kapacitet). Podatci su podijeljeni u dva podskupa: 80 % podataka uzeto je za treniranje, a 20 % za testiranje. Programiranje je provedeno u softveru MATLAB. Rezultati su pokazali da optimiran DA-SVM model s RBF-Gaussovom kernel funkcijom ima dobru sposobnost globalnog pretraživanja uz visoku točnost predviđanja, s $R^2 = 0{,}997$, $R = 0{,}998$ i RMSE = 2,539.
Dobiveni model može se primjenjivati za predviđanje učinkovitosti adsorpcijskog sustava te pruža alat za optimizaciju procesa u skladu s promjenama radnih uvjeta. Razvijeno je novo grafičko korisničko sučelje (GUI) za točnu procjenu željenih odziva koje primjenjuje najbolji DA-SVM model.

Ključne riječi
Višekomponentna adsorpcija, MATLAB GUI, onečišćivala, regresija potpornih vektora, algoritam Dragonfly

[a] *Djilali Bounaama University of Khemis Miliana, Alžir*
[b] *Laboratory of Biomaterials and Transfer Phenomena, University of Médéa, Alžir*
[c] *Quality Control Laboratory, SAIDAL Complex, Médéa Unit, Médéa, Alžir*

Izvorni znanstveni rad
Prispjelo 10. kolovoza 2022.
Prihvaćeno 7. prosinca 2022.